Quantifying Socioeconomic Impact of a Tornado by Estimating Population Outmigration as a Resilience Metric at the Community Level

Hassan Masoomi, S.M.ASCE[1]; John W. van de Lindt, F.ASCE[2]; and Lori Peek, Aff.M.ASCE[3]

Abstract: Policymakers, community leaders, engineers, and researchers have gained interest in understanding tornado-resilient buildings, in part because of the number of deadly and destructive tornadoes over the last decade. In addition to direct losses, such as deaths and damages, tornadoes may also cause many indirect losses as a result of the highly coupled networks within communities. When networks are disrupted, this can cause population outmigration, which, if significant and long-lasting enough, may exacerbate a community's indirect socioeconomic losses over time. In this study, a community was coarsely modeled with its physical-socioeconomic attributes to study population outmigration as a community resilience metric. In this regard, recovery of affected physical networks (i.e., electric power network, water network, and buildings) in the wake of a tornado was investigated and linked to students, household residents, and employees as socioeconomic agents within the community. The probability of outmigration for each household was assessed based on the probability that these three agents in the household are affected over a prescribed time period from the occurrence of the hazard to the full restoration of the community. Finally, the potential population outmigration for the community was assessed by aggregating all the households in the community. The results of such an analysis can be used as a decision-making tool to prioritize hardening of existing infrastructure in a community or optimize master planning of new communities and demonstrates the importance of physical-socioeconomic interactions in resilience studies. **DOI: 10.1061/(ASCE)ST.1943-541X.0002019.**

Author keywords: Tornado; Population outmigration; Population dislocation; Resilient community; Social disruption; Master-planned community.

Introduction

Policymakers, community leaders, engineers, and researchers have expressed growing concern for extreme natural hazard events and the resulting loss of life, property, and economic vitality. One such hazard is supercell-spawned tornadoes that can be in excess of 1 km (0.62 miles) wide and often have long tracks that can pass through an entire community. Recent examples of such events include the Tuscaloosa, Alabama (2011); Joplin, Missouri (2011); and Moore, Oklahoma (2013) tornadoes.

When considering natural hazards in the United States over the last 25 years, tornadoes have caused the third highest number of fatalities, only surpassed by floods and lightning, and the third highest in total dollar losses, just after floods and hurricanes (Boruff et al. 2003). Although the probability that a tornado strikes a particular area of a community is quite low, the consequences can be severe since communities are made up of coupled networks and any malfunction in a part of a network can threaten the functionality of other parts of that network, as well as other networks. Therefore, the functionality of a building depends not only on its own physical performance but also on its supporting networks, including electric power and water. Any disruption in a network can threaten the building occupancy and business continuity. This, in turn, may result in indirect economic losses and population outmigration, two key metrics in assessing the resilience of a community following a disruption.

A resilient community is one that has planned for potential hazards in order to be able to resist, absorb, and adjust to changing conditions, as well as to return to a level of normalcy within a reasonable time following a disaster (Bruneau et al. 2003; Alexander 2013; Platt et al. 2016). A number of metrics have been introduced to represent resilience [e.g., (Bruneau et al. 2003; Bruneau and Reinhorn 2007; Reed et al. 2009; Attoh-Okine et al. 2009; Omer et al. 2009; Henry and Ramirez-Marquez 2012; Ouyang et al. 2012; Ayyub 2014, 2015)]. These metrics have been used in several studies in order to quantify the resilience of, for example, healthcare facilities [e.g., (Cimellaro et al. 2010)]; water networks [e.g., (Chang and Shinozuka 2004); electric power networks [e.g., (Reed et al. 2009; Ouyang and Dueñas-Osorio 2014; Nan and Sansavini 2017)]; and transportation networks [e.g., (Pant et al. 2014)]. In the current study, a socioeconomic resilience metric focused on population outmigration is proposed at the community level.

Population dislocation has been defined as a postdisaster socioeconomic impact in which households are forced to move for some period of time due to damage to structures and infrastructure in the wake of natural disasters (Lindell and Prater 2003;

[1]Ph.D. Candidate, Dept. of Civil and Environmental Engineering, Colorado State Univ., Fort Collins, CO 80523-1372. E-mail: Hassan.Masoomi@colostate.edu

[2]George T. Abell Distinguished Professor in Infrastructure and Co-Director, Dept. of Civil and Environmental Engineering, NIST Center of Excellence for Risk-Based Community Resilience Planning, Colorado State Univ., Fort Collins, CO 80523-1372 (corresponding author). E-mail: jwv@engr.colostate.edu

[3]Professor of Sociology and Director of the Natural Hazards Center, Univ. of Colorado-Boulder, Boulder, CO 80309-0327. E-mail: Lori.Peek@colorado.edu

Note. This manuscript was submitted on March 6, 2017; approved on October 23, 2017; published online on March 14, 2018. Discussion period open until August 14, 2018; separate discussions must be submitted for individual papers. This paper is part of the ***Journal of Structural Engineering***, © ASCE, ISSN 0733-9445.

Mitchell et al. 2012; Xiao and Van Zandt 2011). FEMA (2003), through their *HAZUS* model, proposed a model to measure population dislocation in order to estimate the number of people requiring short-term shelter. The model considers only structural damage and housing type such that all residents in completely damaged (i.e., damage state 4) single-family structures and completely damaged (i.e., damage state 4) multifamily structures, as well as 90% of residents in extensively damaged (i.e., damage state 3) multifamily structures will move after a natural disaster. Lin (2009) modified the *HAZUS* model to consider socioeconomic characteristics of households and their surrounding neighborhoods, in addition to the housing structural damage level and type in estimating population dislocation. The modified model was implemented in *MAEviz* (MAEC 2006), a loss assessment software package developed by the Mid-America Earthquake (MAE) Center and the National Center for Supercomputing Applications (NCSA). Population dislocation was conceptualized in *HAZUS* (FEMA 2003) and *MAEviz* (MAEC 2006) as the households who are forced to leave their homes following a disaster for at least some period of time which may take into account the dislocated households during the preimpact evacuation (Lin 2009).

According to previous disaster studies, population dislocation is a function of several factors including housing structural damage, housing type, disaster type, weather conditions, infrastructure disruption, and loss of employment; these factors are further influenced by socioeconomic characteristics of households and their surrounding neighborhoods (Baker 1991; FEMA 2003; Gladwin and Peacock 1997; Lindell et al. 2006; Whitehead et al. 2000; Whitehead 2005). The population dislocation models used in *HAZUS* (FEMA 2003) and *MAEviz* (MAEC 2006) consider only two and three of the aforementioned factors, respectively, while other factors such as infrastructure disruption and employment loss play key roles in a households' tendency (or decision) to dislocate. These proposed models are reasonable as long as they are used to estimate the number of people requiring short-term shelter. These models, however, do not necessarily offer an accurate representation of resilience in that they only partially meet robustness as a resilience property, while they do not consider the effect of the restoration process (which per se includes the other three properties of resilience—redundancy, resourcefulness, and rapidity) in population dislocation assessment.

The term population dislocation has been used to define the households who stay away from their homes for any period of time, either short term or long term. However, the purpose of the current study is to investigate the population who outmigrate, meaning they dislocate permanently or long enough to have a meaningful effect on indirect economic losses. According to previous studies, the return of households and businesses are mutually dependent (Xiao and Van Zandt 2011). In fact, the return of households in the market area will increase the chances for businesses to return and vice versa. Furthermore, if the displaced households are not included in the U.S. census, the population loss puts the community at risk of losing federal and state funding that are based on a certain threshold for the community's population (Xiao and Van Zandt 2011).

In order to distinguish the current terminology used in this paper from the definition of population dislocation used in the *HAZUS* (FEMA 2003) and *MAEviz* (MAEC 2006) models, *population outmigration* is used in this study to mean the permanent or long-term population loss of a community as a result of households moving because of damage to buildings, infrastructure, school closure, loss of employment, or various combinations thereof, in the aftermath of a natural disaster. The factors that influence population dislocation also affect population outmigration. Therefore, the proposed model is such that the disaster type, weather conditions, and socioeconomic characteristics of households and their surrounding neighborhoods can be included as a parameter describing the households' tendency toward outmigration. It is recognized that this is a significant simplification but does not misrepresent the potential inaccuracies that stem from a dearth of data on this complex topic. In the model, population outmigration is updated during the restoration process until the full restoration of the community is achieved, and it can be assessed at any level (e.g., partial community level and community level).

Illustrative Community Modeling

In order to study community resilience, a simplified community was modeled after Norman, Oklahoma. Since the modeled community does not take into account all aspects of a community, it is not strictly representative of Norman, and therefore, it has been termed *pseudo-Norman* in this study. Residences, businesses, school buildings, the water network, and the electric power network were considered in the model of pseudo-Norman.

Residential Grids

The western part of Norman, with an area of 14.5 by 12.9 km (9 by 8 miles) was studied herein as pseudo-Norman. This area includes more than 90% of Norman's population. The study area was divided into 0.16-km^2 (1/16-mi^2) grids in order to coarsely define the properties of households and businesses in pseudo-Norman with enough detail to still perform the analyses effectively. The number of houses in each grid were counted using *Google Maps*, and the results are shown in Fig. 1(a) as a heat map.

Pseudo-Norman was estimated to have 41,254 houses, which is comparable to 41,813 houses based on the census data in 2013 (City-Data 2016). Then, the number of occupied and unoccupied houses, population, and the number of students at each school level were derived from the census data for each grid and the entire city. Thus, 37,785 occupied houses; 3,469 unoccupied houses; 4,829 elementary school students; 3,671 middle school students; 3,460 high school students; and a total population of 110,844 make up the community of pseudo-Norman.

In order to link the residential grids to business grids (explained later), the employees who live in each residential grid must be associated with a place of employment (termed their *workplace* hereafter) in a business grid. The business grids are shown in Fig. 1(b). It was assumed that each occupied house in the city has two people who are eligible to work, which means that, in total, 75,570 people who live in the city can be an employee. However, based on the census, there is some percentage of unemployment for each grid, which results in 71,198 employees who live in pseudo-Norman. Yet, in the census, only 70% of these employees (i.e., 49,848 employees) work in pseudo-Norman and the rest have a job outside of the city. For each residential grid, those employees who work in the city were divided into 10 groups, and each group was assigned to a business grid. Moreover, as will be discussed later, each residential grid is supplied by specific school buildings, water tower(s), and an electric power distribution substation. Therefore, residential grids are cross-dependent to business grids, the water network, the electric power network, and school buildings in this study. Furthermore, the median household income and the median family income were recorded for each residential grid to consider the household's economic status in the resilience and decision-making analyses.

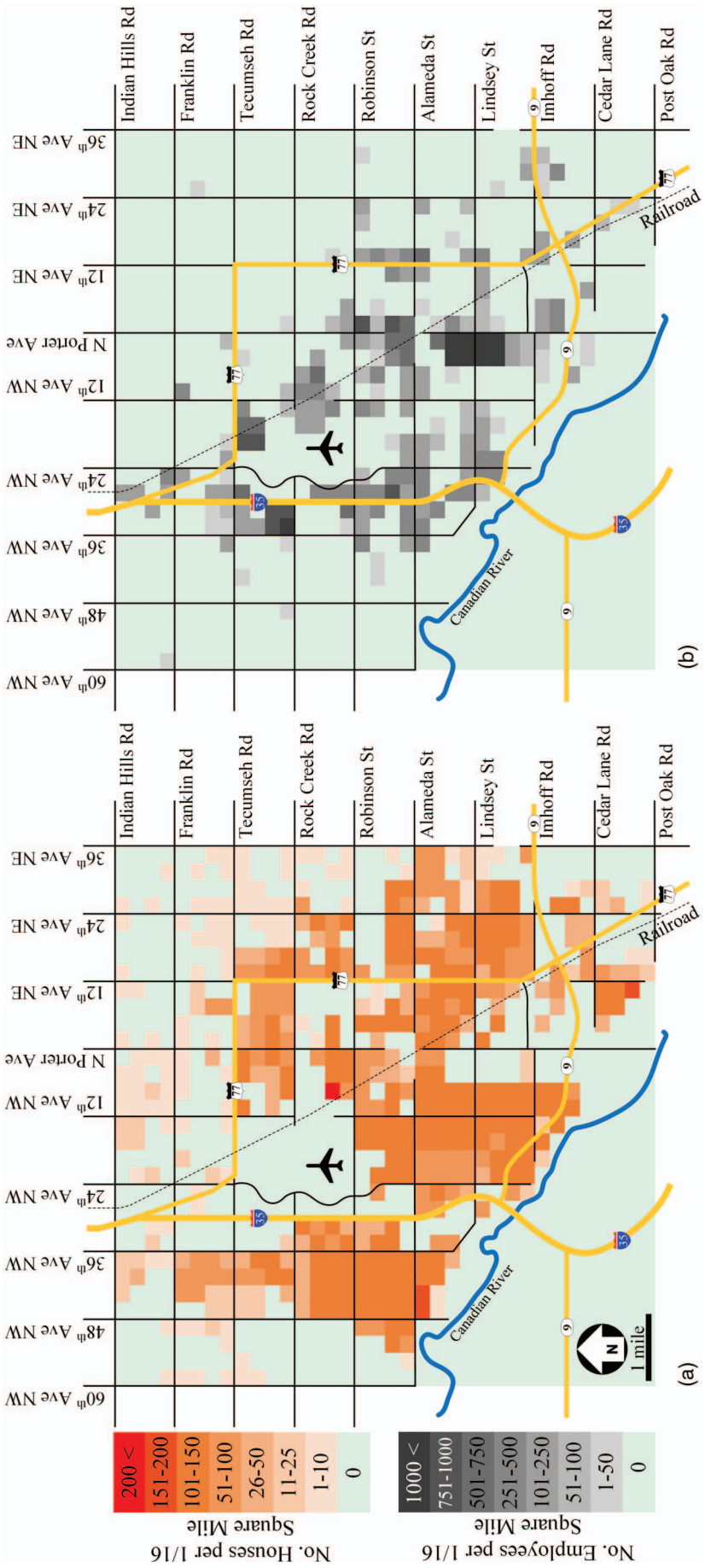

Fig. 1. (Color) Pseudo-Norman map showing (a) the density of residential buildings in residential grids; (b) the number of employees in business grids

Business Grids

The number of workplaces in each grid was also approximately counted. For each workplace, a number of employees were assumed, and the number of employees for each business grid was measured, which is depicted in Fig. 1(b), again as a heat map. In total, 53,890 people work in pseudo-Norman, of which 49,848 employees live in the city and the rest (i.e., 4,042 employees) live outside of pseudo-Norman. As mentioned before, the corresponding residential grids for employees who work in a business grid is known, which can be used to consider the influence of affected businesses on the households and vice versa as will be discussed later.

Each business grid in pseudo-Norman is supplied by specific water tower(s) and an electric power distribution substation. Therefore, business grids are cross-dependent to residential grids, the water network, and the electric power network. Although all the houses in pseudo-Norman were modeled as residential grids, some of the workplaces in business grids that have critical effects on the resilience of the community were defined separately as points in order to be studied more thoroughly for future economic studies. These particular workplaces include hospitals, fire departments, police departments, Walmart, shopping centers, and the airport.

Infrastructure

The water network (WN), the electric power network (EPN), and school buildings are considered for pseudo-Norman in this example. Fig. 2(a) shows the water network and electric power network for the city. The simplified water network includes six water towers (WT) with different capacities and one water treatment plant (WTP). A coverage zone was assumed for each water tower such that a residential/business grid may be covered by more than one water tower. The functionality of each WT depends not only on its physical performance but also on the electric power distribution substation, which provides electricity for its pumping station, as well as on the functionality of the water treatment plant. Therefore, the WN is cross-dependent with the EPN.

The EPN in this study includes 4 transmission substations (TSS), 18 distribution substations (DSS), 123 transmission towers, and 1,393 subtransmission towers. The major part of the EPN is shown in Fig. 2(a). Transmission and subtransmission towers are spaced 310 and 110 m, respectively. The electric power is transferred through buried underground distribution lines to the end users from distribution substations. However, Norman, Oklahoma, has overhead distribution lines, which makes the EPN more vulnerable when subjected to tornadoes. Coverage zones for electric power distribution substations were defined such that each residential/business grid is supplied by only one distribution substation. In other words, although there might be redundancy in providing electricity for a DSS, i.e., several (sub)transmission lines to a DSS, there is no redundant DSS for end users. In the case of tornadoes, uprooted trees may cause damages to underground electric power distribution lines or pipelines of the water network; however, that effect was neglected in the current study.

School buildings (SB) were modeled in the resilience analysis since the destruction of school buildings in natural disasters can not only cause injuries and fatalities but also substantial social disruption following the event (Fothergill and Peek 2015). As shown in Fig. 2(b), 15 elementary schools (ES), 4 middle schools (MS), and 2 high schools (HS) host pseudo-Norman students. The attendance boundary of school buildings is also shown in Fig. 2(b) using different colors [see Masoomi and van de Lindt (2018) for more details], which illustrates the cross-dependency of residential grids and school buildings. Each school building is supplied by a distribution substation and one or more water tower(s). Therefore, school buildings are cross-dependent to the WN and EPN.

Community Components' Properties

After defining the topology of the community, the dependencies among components, and the cross-dependencies between networks, the next step in the analysis was to understand how the community components behave when subjected to a simulated tornado. In this regard, a set of tornado fragility curves corresponding to damage states 1–4 were used to represent the performance of each community component. Additionally, a repair time associated with each damage state for each community component was utilized in order to investigate the restoration process following the simulated tornado.

Tornado Fragility Curves

The residential buildings in pseudo-Norman were categorized into six types including one-story gable-roof wood-frame buildings (two sizes), two-story hip-roof wood-frame buildings, two-story gable-roof wood-frame buildings (two sizes), and mobile homes. Furthermore, seven building types were considered in this study to be representative of business buildings in pseudo-Norman, including industrial buildings (two sizes) (Lee et al. 2013; Koliou et al. 2017); tilt-up precast concrete (i.e., big box) buildings (Koliou et al. 2017); one-story masonry buildings (three sizes); and two-story reinforced concrete buildings.

Moreover, all school buildings in this study were assumed to have masonry construction. High schools were assumed to be one-story reinforced masonry and have one auditorium and two gymnasiums (Masoomi and van de Lindt 2016), while middle schools and elementary schools were modeled as unreinforced masonry buildings with fully grouted and ungrouted construction, respectively. Selection of the level of grouting and reinforcement was arbitrary in this study and intended to represent different design code eras. One auditorium and one gymnasium were considered for the middle schools, while elementary schools had only one long-span multipurpose area. Fragility parameters for DS4 for the components of the electric power network are based on the work done by Lopez et al. (2009), while because of the lack of information, DS1 to DS3 for substations were assumed in this study to have the same logarithmic standard deviation as DS4, but with median wind speed equal to 55, 65, and 80% of the median for DS4, respectively. Moreover, it was assumed that if a transmission or subtransmission tower experiences any structural damage in a tornado, it is replaced with a new tower. This is consistent with the second author's stakeholder interviews with power company personnel. Therefore, only one damage state (i.e., DS4) was assumed for these towers. The fragility parameters for the water network components were assumed by the authors of this study. The fragility parameters, for damage states 1–4, are tabulated in Table 1 for all community components utilized in this study.

Initiation Time and Repair Time

A random variable with Weibull distribution was defined in this study for initiation time, which is the time period following a tornado needed to clean up the debris on roadways, search and rescue, and inspect infrastructure to assess the extent of the damage. It is recognized that this varies significantly, and values herein are based on the second author's experience with postdisaster site

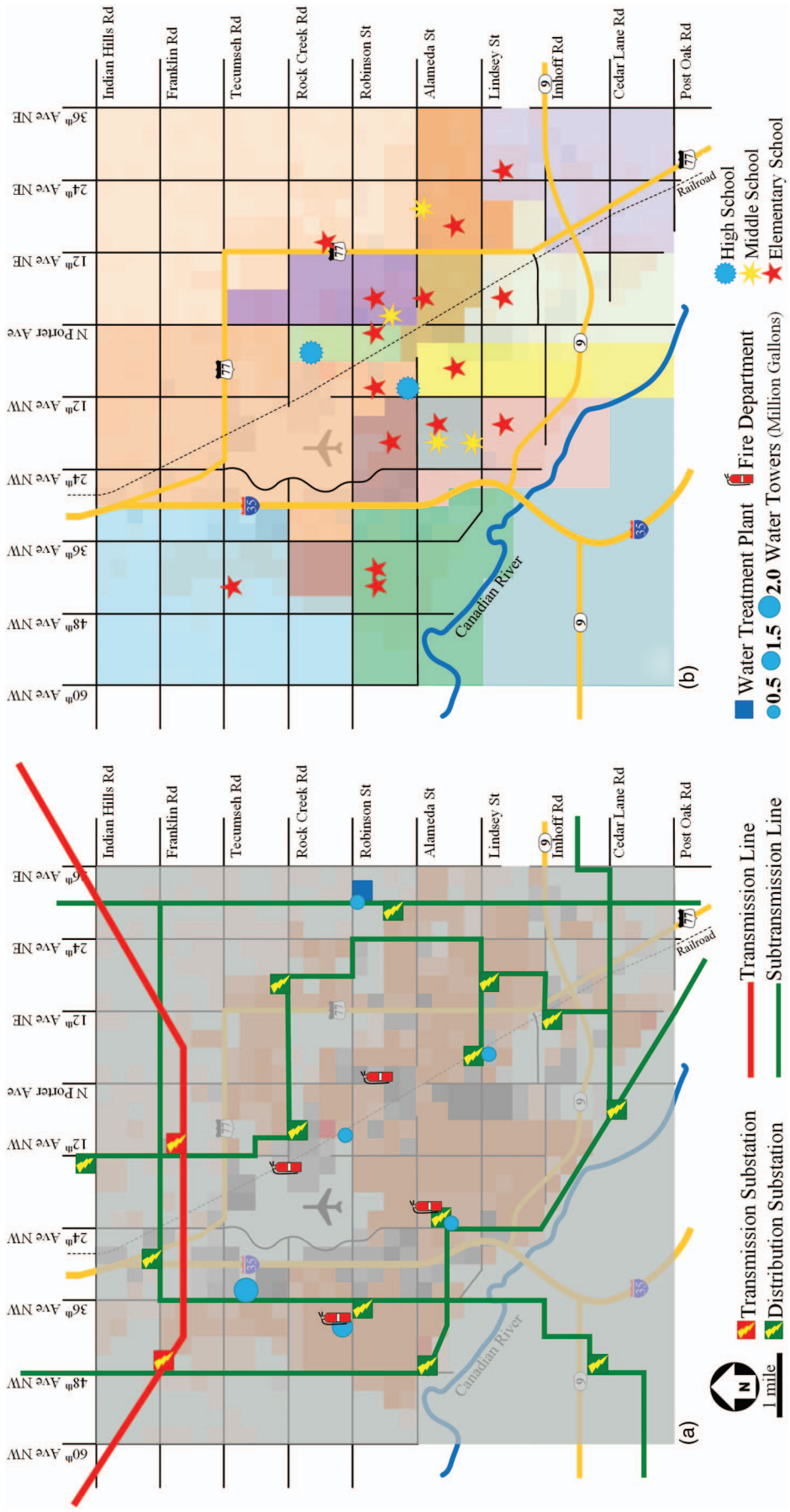

Fig. 2. (Color) (a) Electric power network and water network; (b) public school buildings in pseudo-Norman

Table 1. Fragility Parameters for the Community Components Used in This Study

Network	Component	DS1 Median [m/s (mph)]	DS1 ξ	DS2 Median [m/s (mph)]	DS2 ξ	DS3 Median [m/s (mph)]	DS3 ξ	DS4 Median [m/s (mph)]	DS4 ξ
Residential buildings	Small, one-story	41.1 (91.9)	0.11	49.3 (110.3)	0.11	52.5 (117.4)	0.11	54.8 (122.6)	0.12
	Small, two-story	45.4 (101.6)	0.17	52.3 (117.1)	0.14	54.1 (120.9)	0.12	60.6 (135.5)	0.12
	Medium, one-story	33.2 (74.3)	0.10	37.9 (84.9)	0.10	45.7 (102.3)	0.10	49.1 (109.8)	0.10
	Medium, two-story	37.2 (83.1)	0.15	40.7 (91.1)	0.13	44.3 (99.2)	0.12	48.8 (109.1)	0.14
	Large, two-story	38.2 (85.4)	0.13	42.0 (94.0)	0.11	47.9 (107.1)	0.10	49.5 (110.7)	0.10
	Mobile home	35.5 (79.5)	0.09	42.2 (94.4)	0.09	49.2 (110.0)	0.11	52.7 (117.8)	0.12
Workplace buildings	Small industrial	29.8 (66.7)	0.08	35.7 (79.8)	0.05	38.7 (86.5)	0.06	43.2 (96.5)	0.06
	Large industrial	28.9 (64.7)	0.08	36.8 (82.3)	0.09	69.1 (154.5)	0.11	77.1 (172.4)	0.10
	Big-box	34.0 (75.9)	0.09	41.1 (91.8)	0.08	65.0 (145.5)	0.10	76.3 (170.7)	0.10
	Small unreinforced masonry	31.3 (70.1)	0.09	44.5 (99.5)	0.09	51.2 (114.4)	0.11	64.4 (144.0)	0.23
	Medium unreinforced masonry	39.1 (87.4)	0.09	47.2 (105.6)	0.09	52.7 (117.9)	0.10	79.4 (177.7)	0.12
	Large reinforced masonry	40.6 (90.9)	0.09	47.2 (105.6)	0.11	52.7 (117.9)	0.10	80.2 (179.5)	0.12
	Two-story reinforced concrete	32.3 (72.2)	0.08	40.6 (90.9)	0.09	48.2 (107.8)	0.08	56.0 (125.2)	0.14
School buildings	High school	41.5 (92.8)	0.09	46.3 (103.5)	0.11	52.7 (117.9)	0.10	79.4 (177.7)	0.13
	Middle school	40.6 (90.9)	0.09	47.2 (105.6)	0.11	52.7 (117.9)	0.10	70.4 (157.6)	0.12
	Elementary school	39.1 (87.4)	0.09	47.2 (105.6)	0.09	50.6 (113.3)	0.13	60.6 (135.6)	0.22
Electric power network	Transmission substation and distribution substation	33.4 (74.8)	0.20	39.5 (88.4)	0.20	48.6 (108.8)	0.20	60.8 (136.0)	0.20
	Transmission tower	—	—	—	—	—	—	60.8 (136.0)	0.12
	Subtransmission tower	—	—	—	—	—	—	55.9 (125.0)	0.12
Water network	Water tower	34.4 (77.0)	0.15	40.7 (91.0)	0.15	50.1 (112.0)	0.15	62.6 (140.0)	0.15
	Water treatment plant	36.9 (82.5)	0.15	43.6 (97.5)	0.15	53.6 (120.0)	0.15	67.1 (150.0)	0.15

Note: ξ = log-standard.

Table 2. Statistics for Initiation Time

EF scale	EF0	EF1	EF2	EF3	EF4	EF5
Mean (days)	0.2	0.4	0.8	1.5	2.0	3.0
COV	0.5	0.5	0.5	0.5	0.5	0.5

investigations. The statistics for initiation time are assumed and presented in Table 2.

The occurrence of any damage state in a community component was assumed to disturb the functionality of that component. However, in order to capture the effect of different damage states on functionality, the damage state for each community component was linked to a corresponding repair time. Therefore, the occurrence of a greater damage state in a component means it will take more time to repair, and therefore, it will be nonfunctional for a longer time period.

Table 3 presents the repair time statistics for the community components for damage states 1–4, which are based on a Weibull distribution. The repair time values for buildings, substations, water towers, and the water treatment plant were extracted from FEMA (2003), but a Weibull distribution was fit to the corresponding normal distribution prescribed in FEMA (2003) due to the fact that time is a non-negative variable. Moreover, the values related to DS3 and DS4 for buildings were modified from FEMA (2003) based on the second author's experience with postdisaster site investigations and recovery process. In addition, the permitting time for buildings and repair time for electric power towers were assumed by the authors based on past tornado observation.

Table 3. Repair Time Statistics for Community Components

Network	Component	DS1 Mean (days)	DS1 COV	DS2 Mean (days)	DS2 COV	DS3 Mean (days)	DS3 COV	DS4 Mean (days)	DS4 COV
Residential buildings	Repair time	5	0.2	20	0.2	90	0.2	180	0.2
	Permitting time	2	0.5	7	0.5	14	0.5	30	0.5
Workplace buildings	Repair time	5	0.2	20	0.2	90	0.5	180	0.5
	Permitting time	2	0.5	5	0.5	10	0.5	30	0.5
School buildings	Repair time	5	0.2	20	0.2	180	0.2	730	0.2
	Permitting time	2	0.5	10	0.5	30	0.5	30	0.5
Electric power network	Transmission substation and distribution substation	1	0.5	3	0.5	7	0.5	30	0.5
	Transmission tower	—	—	—	—	—	—	2	0.5
	Subtransmission tower	—	—	—	—	—	—	1	0.5
Water network	Water tower	1.2	0.35	3.4	0.7	104	0.7	165	0.7
	Water treatment plant	0.9	0.35	1.9	0.6	36	0.7	98	0.6

Table 4. Distribution Parameters for Tornado Path Length and Width

	Marginal Weibull parameters				
	Length [km (mi)]		Width [km (mi)]		
EF scale	Scale parameter (A)	Shape parameter (B)	Scale parameter (A)	Shape parameter (B)	Correlation coefficient
EF0	1.155 (0.718)	0.675	0.041 (0.025)	1.043	0.225
EF1	4.299 (2.671)	0.727	0.093 (0.058)	0.943	0.250
EF2	10.484 (6.514)	0.796	0.188 (0.117)	0.912	0.253
EF3	25.533 (15.865)	1.031	0.420 (0.261)	1.004	0.180
EF4	43.448 (26.997)	1.117	0.703 (0.437)	1.150	0.307
EF5	61.274 (38.074)	1.291	0.921 (0.572)	1.423	0.367

Tornado Path Simulation

The gradient method (Standohar-Alfano and van de Lindt 2014; Masoomi and van de Lindt 2018, 2017) was used in this study to simulate the tornado path. A tornado path is defined by its center coordinate, direction, length, and width. Although each of these parameters can be considered as a random variable, only tornado path length and width were considered as random variables in the current study with the statistics presented in Table 4. Since the tornado path length and width are correlated random variables with known marginal distributions, the Gaussian copula model (Limbourg et al. 2007) was utilized in this study in order to generate the correlated random deviates. An EF4 tornado path with randomly generated length and width, based on the statistics provided in Table 4, is shown as an example in Fig. 3. All the simulated tornado paths in this study had the same direction and center point shown for the EF4 tornado in Fig. 3 but had random width and length based on the statistical distributions provided in Table 4 for each EF scale.

Restoration Analysis

Monte Carlo simulation was conducted in this study to investigate the restoration and resilience analyses for pseudo-Norman

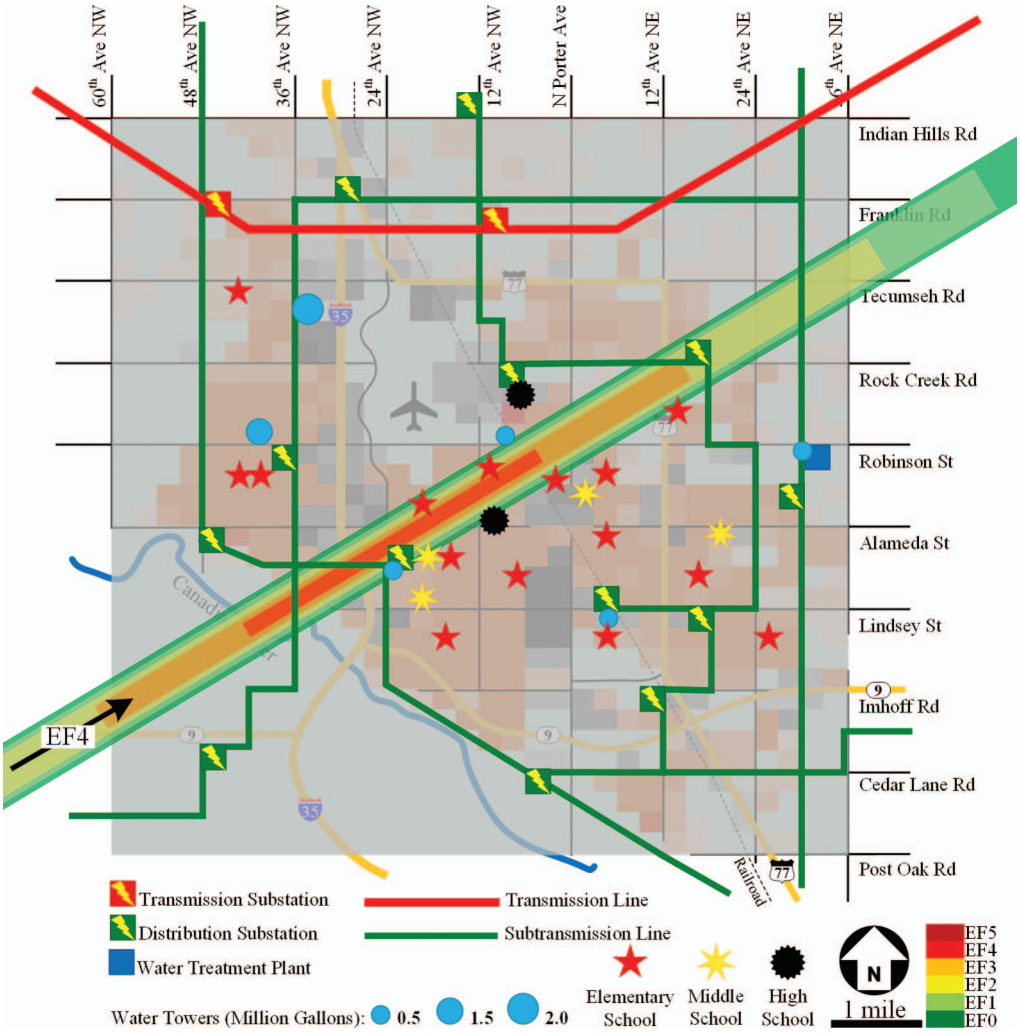

Fig. 3. (Color) Simulated EF4 tornado path through pseudo-Norman

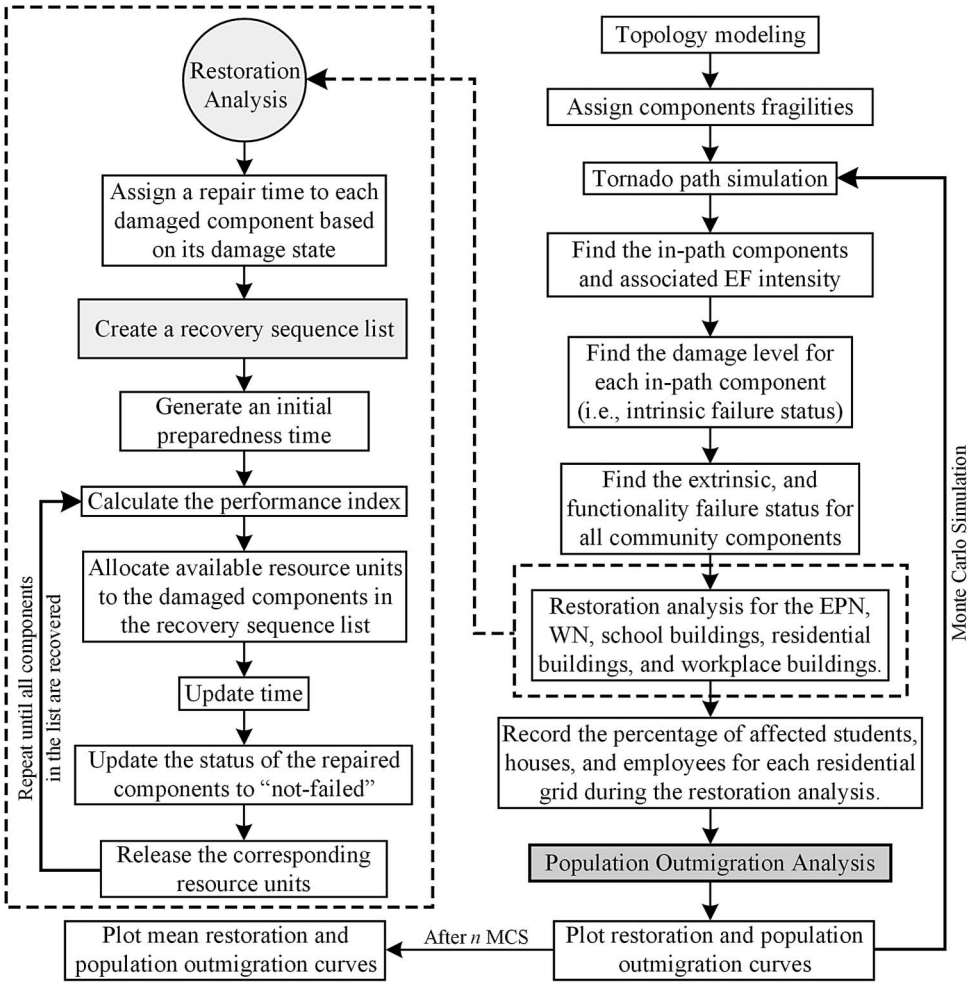

Fig. 4. Steps toward the restoration and population outmigration analyses and the flowchart for the restoration analysis

subjected to tornadoes with a path center and direction as shown in Fig. 3. The analysis was performed for each EF scale tornado with 10,000 random samples of the tornado path with correlated widths and lengths. The fundamental steps of the present study are summarized in Fig. 4. For each tornado path sample, the in-path community components were identified, with the associated tornado intensity acting on them based on their location through the path. Then, in order to simulate the damage level (i.e., no damage, DS1, DS2, DS3, or DS4) for each in-path component, a random deviate, generated based on the standard uniform distribution, was compared to the probabilities for DS1 to DS4 at the tornado intensity acting on the component. After determining the damage level for each component, their intrinsic failure status is available, which is either failed (0 for components with damage level of DS1, DS2, DS3, or DS4) or not failed (1 for components without any damage). Moreover, since it was assumed that the occurrence of any DS results in the failed status (0) for a component, in order to capture the effect of different damage levels in the analyses, repair and permitting times were assigned to each damaged component based on its damage level and the statistics provided in Table 3. The occurrence of a greater damage state in a component means it will take more time to repair, and therefore, it will be nonfunctional for a longer period of time. In other words, damage levels were essentially translated into the time domain for restoration analysis and a higher damage level results in a longer repair time.

The intrinsic failure event for a component is defined as the failure based on its own physical damage level experienced under a simulated tornado, which in this study is considered to be either failed (0 for components with damage level of DS1, DS2, DS3, or DS4) or not failed (1 for components without damage). Then, based on the intrinsic failure status of all the community components, as well as their dependencies and cross-dependencies, the extrinsic failure status and functionality status can be found for each component. The extrinsic failure event for a component is defined as the failure that results when interacting components outside of the component are considered either within its own network or other networks in the community. The functionality failure event for a component is the union of the intrinsic and extrinsic failure events for that component, which can be expressed as

$$F_{fnc} = F_{int} \cup F_{ext} \tag{1}$$

where F_{fnc}, F_{int}, and F_{ext} = functionality, intrinsic, and extrinsic failure events for a component, respectively.

A specified performance index at a network level or at the community level can be assessed when the functionality status of all community components is known. As will be discussed later, the restoration process is simulated by updating the specified performance index over time steps after the simulated tornado until full restoration of the community is achieved. In the restoration analysis, it was assumed that the repair process of all networks can be started simultaneously immediately after the initiation time.

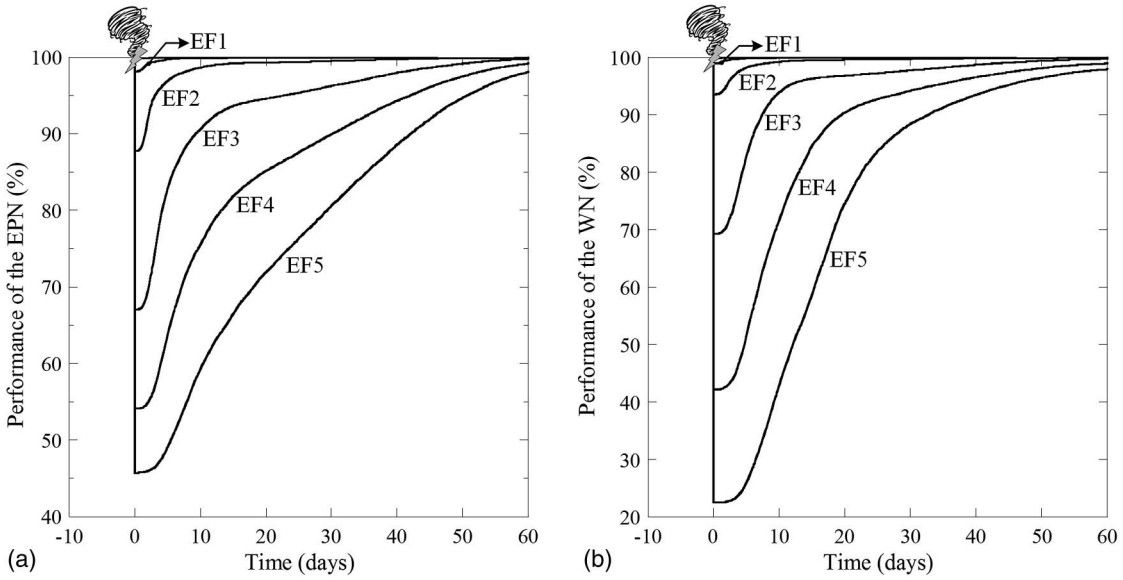

Fig. 5. Restoration curves for (a) electric power network and (b) water network after tornadoes with the path center and direction shown in Fig. 3 and with different intensities

Electric Power Network

The electric power network plays a substantial role in the vitality of a community in that the functionality of all other networks depends on the availability of electric power. Many critical facilities such as hospitals and police stations do have generators, but this particular subcomponent was neglected in the present study. The focus was on the methodology development to examine restoration with interdependencies and particular cross-dependencies between sectors in place. The EPN in this study has underground distribution lines, which are assumed to be undamaged from a tornado. Therefore, the electric power distribution substations (DSS) are the supplier nodes for demand nodes of other networks, which means the functionality status of DSSs dictates the extrinsic failure status of demand nodes. The extrinsic failure status and functionality status of each DSS were investigated by considering the dependency among the EPN components. An adjacency matrix was used to find all the paths that transfer electricity to each DSS. The extrinsic failure status is 0 if all the paths that end at the DSS have at least one failed component; otherwise, the status is 1, which can be expressed mathematically as

$$P\left(F_{fnc}^{DSS_i}\right) = P\left(F_{int}^{DSS_i} \cup F_{ext}^{DSS_i}\right) = P\left[F_{int}^{DSS_i} \cup \left(\bigcap_{j=1}^{n} F_{fnc}^{path_j}\right)\right] \tag{2}$$

where $F_{fnc}^{DSS_i}$, $F_{int}^{DSS_i}$, and $F_{ext}^{DSS_i}$ = functionality, intrinsic, and extrinsic failure events for the distribution substation i, respectively, and $F_{fnc}^{path_j}$ = functionality failure event of the path j, which provides electricity for the DSS_i.

In this study, a constraint for available recovery resource units, as well as a recovery priority, was considered in the restoration process of the EPN, while all the damaged components in the other networks were assumed to be repaired with no constraint or prioritization rules. Five available resource units, r, as generic work teams, including repair crews, equipment, and replacement components, were considered for assignment to damaged components in the EPN (Ouyang et al. 2012). Moreover, the recovery priority in the EPN was considered such that a DSS with a higher demand has to be restored first. Since there are redundancies in some DSSs, the path with the shortest recovery time was selected to be restored first. The restoration process for the EPN is explained in detail by Masoomi and van de Lindt (2018). The performance index for the EPN was defined as the percentage of the community demand being supplied by the EPN. A Monte Carlo simulation was implemented to obtain the average performance of the EPN in the restoration process, which is shown in Fig. 5(a) for all EF scales.

Water Network

In the water network (WN), the water towers (WT) are the supplier nodes. Each WT has a pumping station that links the WN to the supplier nodes in the EPN (i.e., the DSSs). The functionality of the water treatment plant (WTP) has a direct effect on the extrinsic failure status of the water towers. Therefore, the functionality failure probability for the WTs can be expressed as

$$P\left(F_{fnc}^{WT_i}\right) = P\left(F_{int}^{WT_i} \cup F_{ext}^{WT_i}\right) \tag{3}$$

$$F_{ext}^{WT_i} = F_{fnc}^{WTP} \cup F_{fnc}^{DSS_j} = \left(F_{int}^{WTP} \cup F_{ext}^{WTP}\right) \cup F_{fnc}^{DSS_j} \tag{4}$$

where $F_{fnc}^{WT_i}$, $F_{int}^{WT_i}$, and $F_{ext}^{WT_i}$ = functionality, intrinsic, and extrinsic failure events for the water tower i, respectively, and F_{fnc}^{WTP}, F_{int}^{WTP}, and F_{ext}^{WTP} = functionality, intrinsic, and extrinsic failure events for the water treatment plant, respectively. F_{ext}^{WTP} is equivalent to the functionality failure event for the DSS that feeds the WTP, and $F_{fnc}^{DSS_j}$ is the functionality failure event for the distribution substation that feeds WT_i.

The performance index for the water network is defined as the percentage of the community demand being supplied by the WN. The average performance of the WN following the tornado is shown in Fig. 5(b) for all EF scales. For the EPN and WN, there exist portable substations and portable water treatment systems, respectively. At this time, these are not being included in the analysis but may be considered in future studies.

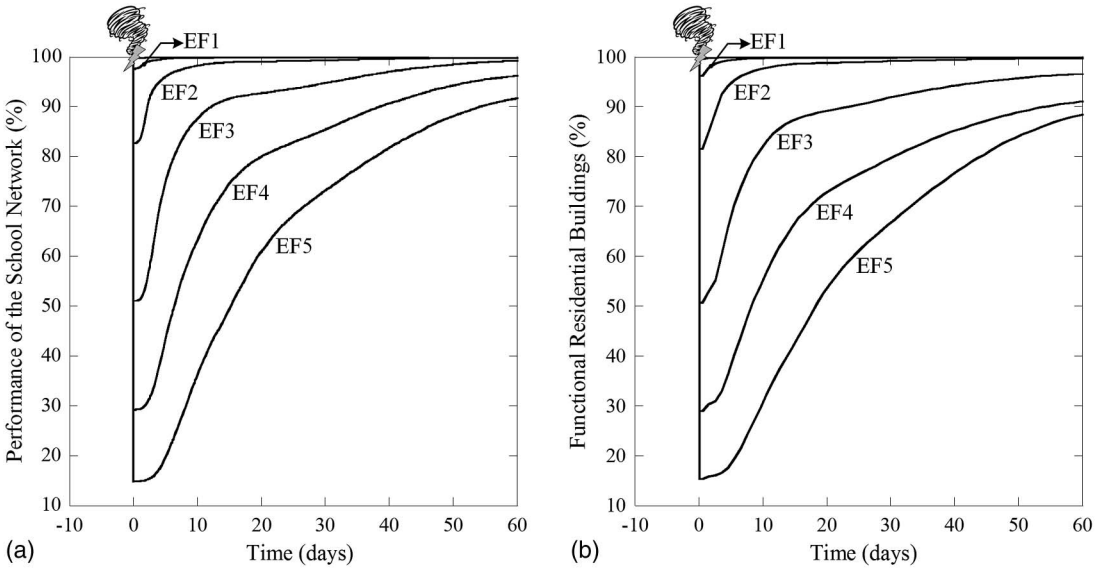

Fig. 6. Restoration curves for (a) school network and (b) residential buildings after tornadoes with the path center and direction shown in Fig. 3 and with different intensities

School Network

The functionality of a school building was modeled to be a function of its own physical performance, as well as the availability of both water and electric power. Electric power is provided for a component by one specific distribution substation. However, it was assumed that the water can be delivered to a component from several water towers, i.e., some level of redundancy. The pressure in pipelines was not considered in the determination of availability of water for a component. It was assumed that the water demand for a component was not satisfied under the condition that all water towers capable of supplying that component lost functionality. Therefore, the functionality failure probability for a school building (SB) can be defined as

$$P\left(F_{fnc}^{SB_i}\right) = P\left(F_{int}^{SB_i} \cup F_{ext}^{SB_i}\right) \tag{5}$$

$$F_{ext}^{SB_i} = F_{fnc}^{DSS_j} \cup \left(\bigcap_{k=1}^{k=n} F_{fnc}^{WT_k}\right) \tag{6}$$

where $F_{fnc}^{SB_i}$, $F_{int}^{SB_i}$, and $F_{ext}^{SB_i}$ = functionality, intrinsic, and extrinsic failure events for school building i, respectively; $F_{fnc}^{DSS_j}$ = functionality failure event for the distribution substation that feeds SB_i; and $F_{fnc}^{WT_k}$ = functionality failure events for the n water towers that provide water for SB_i.

The performance index for the school network is defined as the percentage of a community's students that can be served by the school network. The average performance of the school network during its restoration process is shown in Fig. 6(a) for all EF scales. Moreover, the percentage of affected students in each residential grid (RG), $P_S(t, RG_i)$, was calculated and recorded during the restoration process in order to be considered in the population outmigration analysis. An affected student is defined herein as a student whose school is nonfunctional.

Residential Buildings

The functionality of a residential building (RB) is considered the same way as the school building, which is expressed mathematically in Eqs. (5) and (6). A community-level performance index for the residential buildings is defined as the percentage of functional residential buildings. As mentioned before, pseudo-Norman has 41,254 residential buildings, of which 37,785 buildings are occupied and the rest are unoccupied. The average performance of community residential buildings during the community restoration process was assessed and is shown in Fig. 6(b). For a tornado path with the position shown in Fig. 3 through pseudo-Norman, only a few unoccupied residential buildings (e.g., 25 unoccupied buildings on average for an EF4 tornado) are located in the tornado path. Therefore, the restoration curves shown in Fig. 6(b) appear the same for all the residential buildings as well as only the occupied residential buildings. Furthermore, the percentage of affected (i.e., nonfunctional) occupied residential buildings for each RG, $P_{OR}(t, RG_i)$, was calculated and recorded during the restoration process in order to be considered in the population outmigration analysis. The level of structural damage is one of the factors that affects population dislocation and outmigration. Therefore, the percentage of occupied residential buildings in each damage state can be calculated and recorded for each residential grid at this stage in order to better estimate the population outmigration. However, in the current study, this was neglected, and the occurrence of any damage state was assumed to result in a nonfunctional building in order to focus more on the methodology.

Workplace Buildings

A workplace building (WB) is defined herein as any building type that can employ residents of pseudo-Norman, which has the same functionality failure probability as expressed in Eqs. (5) and (6). A community-level performance index for the workplace buildings is defined as the percentage of employees who work in pseudo-Norman and are not affected by the loss of functionality of workplace buildings. The average performance during the community restoration process was evaluated and is shown in Fig. 8(a). Moreover, the percentage of affected employees who live in each RG, $P_E(t, RG_i)$, was calculated and recorded during the restoration process in order to be considered in the population outmigration analysis. An affected employee is defined herein as an employee whose workplace is nonfunctional.

Businesses Continuity

Although the performance index defined above in the workplace buildings' restoration description can be used to outline an economic resilience metric, perhaps a better index may be used to express business continuity at the community level. In this regard, business continuity was linked not only to the functionality of workplace buildings but also to the employees whose house was physically damaged (e.g., DS1 to DS4) during the tornado.

Fig. 7 sheds light on the cross-dependencies between residential grids and business grids. For example, 70% of the employees whose houses are located in the residential grid marked with a black star in Fig. 7(a) work in a workplace located in the business grids marked with white stars in Fig. 7(b), and the other 30% work outside of the city. Moreover, the employees who work in the business grid marked with a white circle in Fig. 7(b) live in a house located in the residential grids marked with black circles in Fig. 7(a). Some of the employees who work in a business grid may live outside of the city.

The mean number of employees who work in business grid j (BG_j) and whose house experienced damage (i.e., DS1 to DS4), can be expressed as

$$N_E(BG_j|\text{damaged house}) = \sum_{i=all\,RG}\left[\left(\frac{n_E(RG_i \rightarrow BG_j)}{Tn_E(RG_i)}\right)\left(\frac{n_{DOR}(RG_i)}{n_{OR}(RG_i)}\right)Tn_E(RG_i)\right] \quad (7)$$

where $n_E(RG_i \rightarrow BG_j)$ = number of employees who live in residential grid i and work in business grid j; $Tn_E(RG_i)$ = total number of employees who live in residential grid i; $n_{DOR}(RG_i)$ = number of damaged occupied residential buildings (i.e., DS1-DS4) in residential grid i; and $n_{OR}(RG_i)$ = total number of occupied residential buildings in residential grid i.

Then, based on the nonfunctional workplaces in business grid j and the number of employees for each workplace, the number of employees whose workplace is nonfunctional was calculated, $N_E(BG_j|\text{nonfunctional workplace})$. Therefore, the affected businesses were defined based on the calculation of the number of employees whose workplace is nonfunctional or whose house is damaged. The probability that an employee, E, in business grid j is influenced by either a damaged house (DH) or nonfunctional workplace (nfncWP) can be calculated as

$$\begin{aligned} P\left(E_{nfncWP\,or\,DH}^{BG_j}\right) &= P\left(E_{nfncWP}^{BG_j} \cup E_{DH}^{BG_j}\right) \\ &= P\left(E_{nfncWP}^{BG_j}\right) + P\left(E_{DH}^{BG_j}\right) \\ &\quad - P\left(E_{nfncWP}^{BG_j}\right) \cdot P\left(E_{DH}^{BG_j}\right) \end{aligned} \quad (8)$$

$$P\left(E_{nfncWP}^{BG_j}\right) = \frac{N_E(BG_j|\text{nonfunctional workplace})}{Tn_E(BG_j)} \quad (9)$$

$$P\left(E_{DH}^{BG_j}\right) = \frac{N_E(BG_j|\text{damaged house})}{Tn_E(BG_j)} \quad (10)$$

where $P(E_{nfncWP}^{BG_j})$ = probability that an employee in business grid j (BG_j) is affected by a nonfunctional workplace; $P(E_{DH}^{BG_j})$ = probability that an employee in BG_j is affected by a damaged house; $N_E(BG_j|\text{nonfunctional workplace})$ = number of employees in BG_j who are affected by a nonfunctional workplace; $N_E(BG_j|\text{damaged house})$ = number of employees in BG_j who are affected by a damaged house; and $Tn_E(BG_j)$ = total number of employees who work in BG_j.

Then, the business continuity at the community level, which is presented in Fig. 8(b), can be calculated as

$$\text{Business Continuity} = 1 - \frac{\sum_{j=all\,BG}\left[Tn_E(BG_j) \cdot P\left(E_{nfncWP\,or\,DH}^{BG_j}\right)\right]}{Tn_E(\text{pseudo-Norman})} \quad (11)$$

where $Tn_E(BG_j)$ = total number of employees who work in BG_j; $E_{nfncWP\,or\,DH}^{BG_j}$ = probability that an employee in BG_j is affected by either a damaged house or a nonfunctional workplace; and $Tn_E(\text{pseudo-Norman})$ = total number of employees who work in pseudo-Norman. Of course, some employees with a damaged house may still report to their place of employment. At this time in the analysis development, this is neglected, but it will be examined in future studies.

Population Outmigration

Population dislocation, and therefore population outmigration, may occur because of housing structural damage, housing type, disaster type, weather conditions, infrastructure disruption, loss of employment, and myriad other socioeconomic characteristics of individuals and households (Baker 1991; Gladwin and Peacock 1997; Whitehead et al. 2000; Whitehead 2005). In this study, for each household in a residential grid, three parameters were considered to potentially stimulate a household to leave the city with some probability assigned to each and their combinations: (1) affected house (i.e., a nonfunctional house as defined earlier); (2) affected employee (i.e., an employee member of the household whose workplace is nonfunctional); and (3) affected student (i.e., a student member of the household whose school is nonfunctional). These three parameters include building structural damage; disruption of infrastructure (i.e., electric power network, water network, and school network); and employment loss. Based on these three parameters, a household experiences one of eight states (i.e., S1–S8, which are mutually exclusive and collectively exhaustive), as shown in Fig. 9. Each state leads to a different probability of outmigration for the household, which is a function of time, the level of structural damage, housing type, disaster type, weather conditions, household income, race/ethnicity, tenancy status, and so on. For example, a household is assumed to have a greater tendency to outmigrate when state S8 occurs than state S3, and the longer the household sustains a state, the more likely they are to outmigrate. Households residing in multifamily structures are more prone to dislocation (and therefore outmigration) than those living in single-family dwellings, and this vulnerability is even more significant for households inhabiting mobile homes (Peacock and Girard 1997; Lin 2009).

The disaster type can further influence the household's probability of outmigration in that, for example, in the case of a flood, households may have to leave their house if it is in the flooded area regardless of the level of damage. Population outmigration can be exacerbated by weather conditions since utility disruption affects the ability to heat or cool the house. In very cold or hot weather conditions, this may significantly decrease the tolerance of households and therefore increase their probability of dislocation followed by outmigration. A household's socioeconomic status is one of the factors that influences the household's probability of outmigration. Households with higher socioeconomic status have more potential for mobility following a natural disaster, meaning

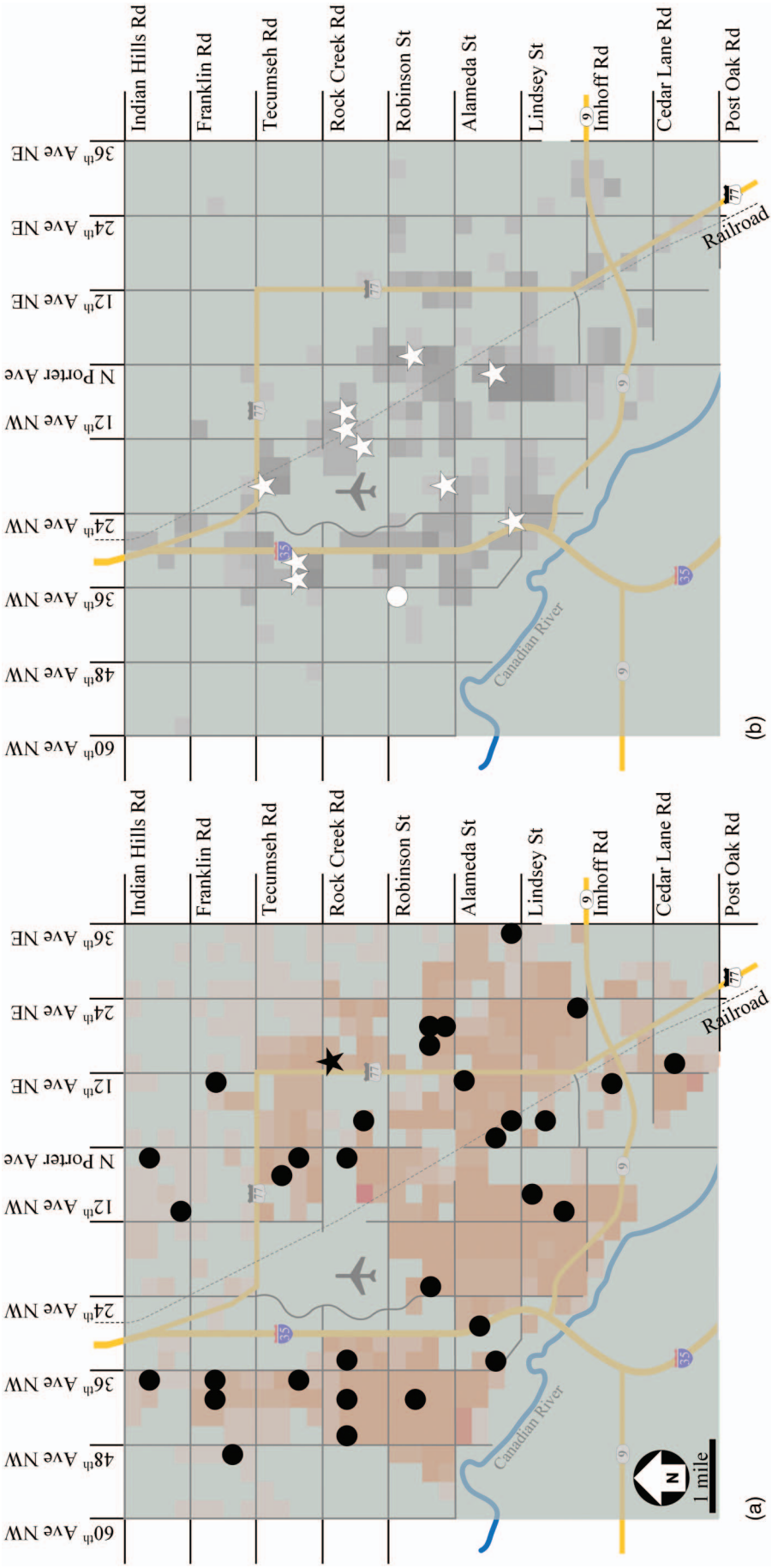

Fig. 7. (Color) Example of cross-dependencies between residential grids and business grids: (a) residential grids; (b) business grids

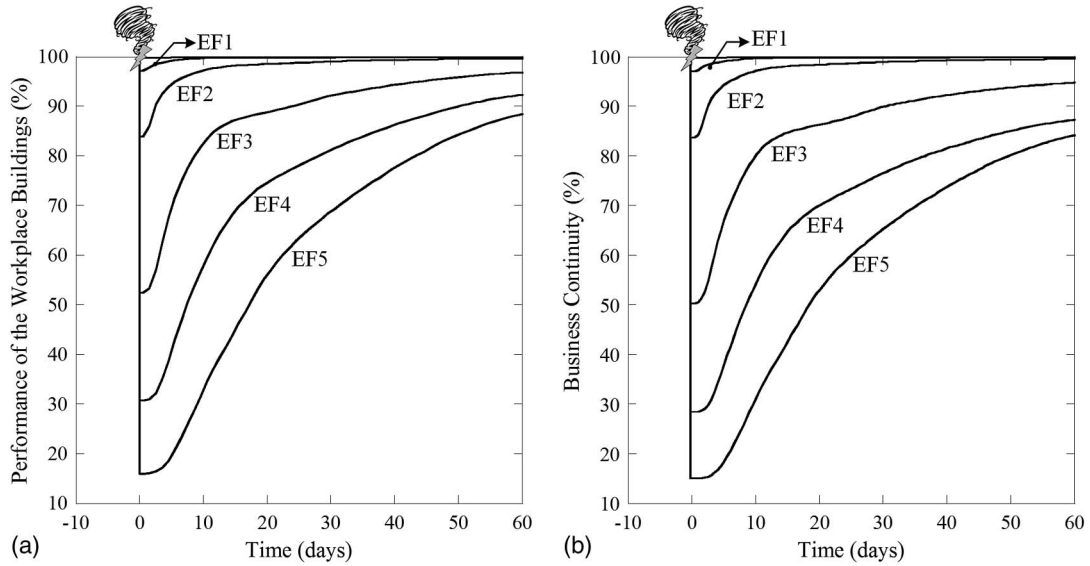

Fig. 8. Restoration curves for (a) workplace buildings and (b) business continuity after tornadoes with the path center and direction shown in Fig. 3 and with different intensities

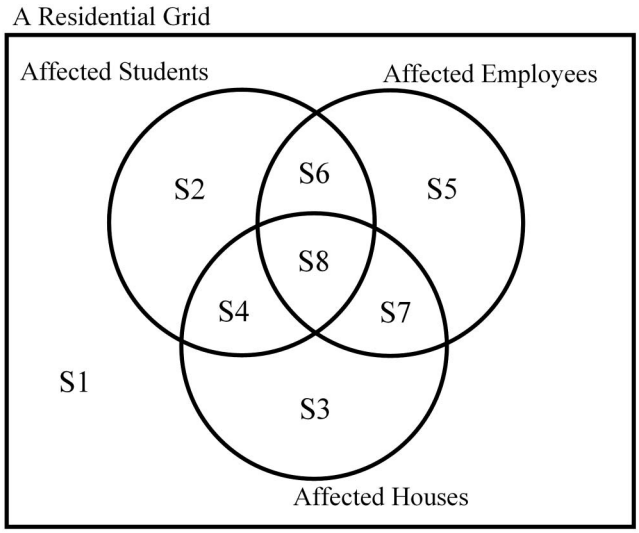

Fig. 9. Venn diagram showing the possible states of a household after an event

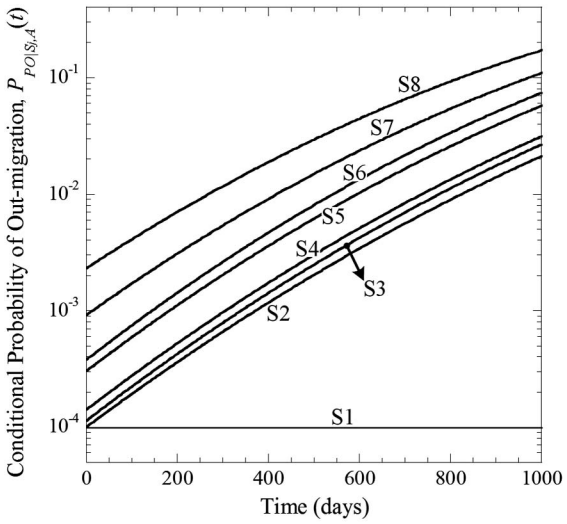

Fig. 10. Household's conditional probability of outmigration as a function of time given that state S_j occurred for the household and, also, the household has not outmigrated until time t

they have more resources to both choose to relocate elsewhere, as well as to rebuild should they so choose (Drabek and Key 1984; Weber and Peek 2012). Moreover, tenancy status of households was found to have an inconsistent effect on household dislocation/outmigration (Peacock and Girard 1997; Belcher and Bates 1983). All the aforementioned factors should be considered in the household's probability of outmigration. However, in the present study, a normal distribution only as a function of time was assumed for the conditional probability of outmigration for each state, given that the household has not outmigrated until that time, which is shown in Fig. 10, in order to illustrate the methodology to quantify population outmigration. Even if a household is not affected by the three parameters (affected house, affected employee, and affected student), i.e., the state S1, a very low constant probability was considered for the household outmigration.

For each RG, the percentage of affected students, $P_S(t, RG_i)$; the percentage of affected occupied residential buildings, $P_{OR}(t, RG_i)$; and the percentage of affected employees, $P_E(t, RG_i)$, were recorded as a function of time during the restoration analysis. Then, the probability that household k (H_k) in residential grid i (RG_i) experiences a state can be calculated at time t as

$$P_{S1}(t, H_k, RG_i) = (1 - P_{OR}(t, RG_i)) \times (1 - P_S(t, RG_i))^{n_S(H_k)} \times (1 - P_E(t, RG_i))^{n_E(H_k)} \quad (12)$$

$$P_{S2}(t, H_k, RG_i) = (1 - P_{OR}(t, RG_i)) \times [1 - (1 - P_S(t, RG_i))^{n_S(H_k)}] \times (1 - P_E(t, RG_i))^{n_E(H_k)} \quad (13)$$

$$P_{S3}(t, H_k, RG_i) = (P_{OR}(t, RG_i)) \times (1 - P_S(t, RG_i))^{n_S(H_k)} \times (1 - P_E(t, RG_i))^{n_E(H_k)} \quad (14)$$

$$P_{S4}(t, H_k, RG_i) = (P_{OR}(t, RG_i)) \times \left[1 - (1 - P_S(t, RG_i))^{n_S(H_k)}\right] \times (1 - P_E(t, RG_i))^{n_E(H_k)} \quad (15)$$

$$P_{S5}(t, H_k, RG_i) = (1 - P_{OR}(t, RG_i)) \times (1 - P_S(t, RG_i))^{n_S(H_k)} \times \left[1 - (1 - P_E(t, RG_i))^{n_E(H_k)}\right] \quad (16)$$

$$P_{S6}(t, H_k, RG_i) = (1 - P_{OR}(t, RG_i)) \times [1 - (1 - P_S(t, RG_i))^{n_S(H_k)}] \times [1 - (1 - P_E(t, RG_i))^{n_E(H_k)}] \quad (17)$$

$$P_{S7}(t, H_k, RG_i) = (P_{OR}(t, RG_i)) \times (1 - P_S(t, RG_i))^{n_S(H_k)} \times [1 - (1 - P_E(t, RG_i))^{n_E(H_k)}] \quad (18)$$

$$P_{S8}(t, H_k, RG_i) = (P_{OR}(t, RG_i)) \times [1 - (1 - P_S(t, RG_i))^{n_S(H_k)}] \times [1 - (1 - P_E(t, RG_i))^{n_E(H_k)}] \quad (19)$$

where $n_S(H_k)$ = number of student members of the household k and $n_E(H_k)$ = number of employee members of the household k.

Therefore, based on the conditional probability of outmigration for each state shown in Fig. 10, the conditional probability of outmigration for the household k at time t given that they have not outmigrated until time t (condition A) can be calculated as

$$P_{PO|A}(t, H_k, RG_i) = \sum_j [P_{PO|S_j,A}(t) P_{S_j}(t, H_k, RG_i)] \quad (20)$$

where $P_{Sj}(t, H_k, RG_i)$ = probability that household k in residential grid i is in state S_j at time t and $P_{PO|Sj,A}(t)$ = household's conditional probability of outmigration at time t if state S_j occurred for the household and the household has not outmigrated until that time, which is shown in Fig. 10.

In order to calculate the probability of outmigration for household k, $P_{PO|A}(t, H_k, RG_i)$ serves as the hazard function for the household outmigration in time-dependent reliability analysis. Therefore, the probability of outmigration for household k in (0,t] can be expressed as

$$P_{PO}(T \le t, H_k, RG_i) = 1 - \exp\left[-\int_0^t P_{PO|A}(\xi, H_k, RG_i) d\xi\right] \quad (21)$$

Finally, the mean percentage of population outmigration for pseudo-Norman can be expressed as

$$PO(T \le t, \text{pseudo-Norman}) = \frac{\sum_i \sum_k [n_{H_k} \cdot P_{PO}(T \le t, H_k, RG_i)]}{\text{Population (city)}} \quad (22)$$

where n_{Hk} = number of people in household k and Population (city) = total number of people in pseudo-Norman.

The population outmigration analysis was performed for pseudo-Norman subjected to tornadoes with different intensities and the path center and direction shown in Fig. 3. The average results of Monte Carlo simulation analyses for population outmigration are shown in Fig. 11 at the grid level and in Fig. 12 at the community level.

As Fig. 11 shows, although a tornado path hits only a small part of the city (a path with the mean width and length is shown in Fig. 11), the entire city is susceptible to the effects of the tornado because of the dependencies and cross-dependencies across components and networks. Fig. 11 shows that even a residential grid outside of the tornado path might have the highest number of outmigrated people among all the grids in the city; e.g., their place of work and school were both destroyed and were nonfunctional for a long period of time.

Fig. 12 shows the cumulative population outmigration (on average) for pseudo-Norman as the percentage of the community's population (i.e., 110,844) following a tornado that strikes pseudo-Norman with the path center point and direction as shown in Fig. 3. In the case of an EF3 tornado, 2.163% of the pseudo-Norman population (approximately 2,400 people) out-migrate as a result of physical-socioeconomic disruptions in the community.

Summary and Conclusion

In this study, population outmigration was defined as a socioeconomic resilience metric, and a model was proposed to quantify the metric either at the grid level or at the community level. In this regard, an illustrative community made up of an electric power network, a simplified water network, school buildings, residential grids, and business grids were modeled, and damages to community components resulting from a tornado were assessed. Then, the functionality of residential buildings, school buildings, and workplace buildings was assessed during the restoration process as a function of the physical damage to buildings and the availability of electric power and water. The affected students, employees, and occupied residential buildings were linked to each household during the restoration analysis, and the probability of outmigration for each household was assessed at evenly spaced time periods after the event until the full restoration of the community was achieved. Finally, the population outmigration was measured as the product of the number of people in the household and the probability of outmigration for all the households in the community.

The results show that the entire city may be substantially affected by a tornado even though it strikes only part of the city. Moreover, it is possible for population outmigration to be higher in a grid outside of the tornado path, which highlights dependencies and cross-dependencies in and among networks. It is recognized that the probability matrix for outmigration was assigned based on logic and not data, so the emphasis in this paper is placed on the methodology, understanding that an extensive postdisaster survey would need to be conducted to complete the outmigration probability matrix.

This study has two main implications for future studies. First, it can be used in analyses supporting risk-informed decision making in order to design master-planned resilient communities, as well as upgrading a community's buildings and/or infrastructure to make the community more resilient to future disasters. This could, for example, be used to understand how to better isolate or decouple two or more sectors; establish redundancies; or decide whether to focus on retrofitting schools in the public sector, businesses and residences in the private sector, or some combination thereof. Second, the population outmigration derived in this study can be further utilized to update the business continuity in a community in that these two metrics (i.e., population outmigration and business continuity) have an inverse relationship.

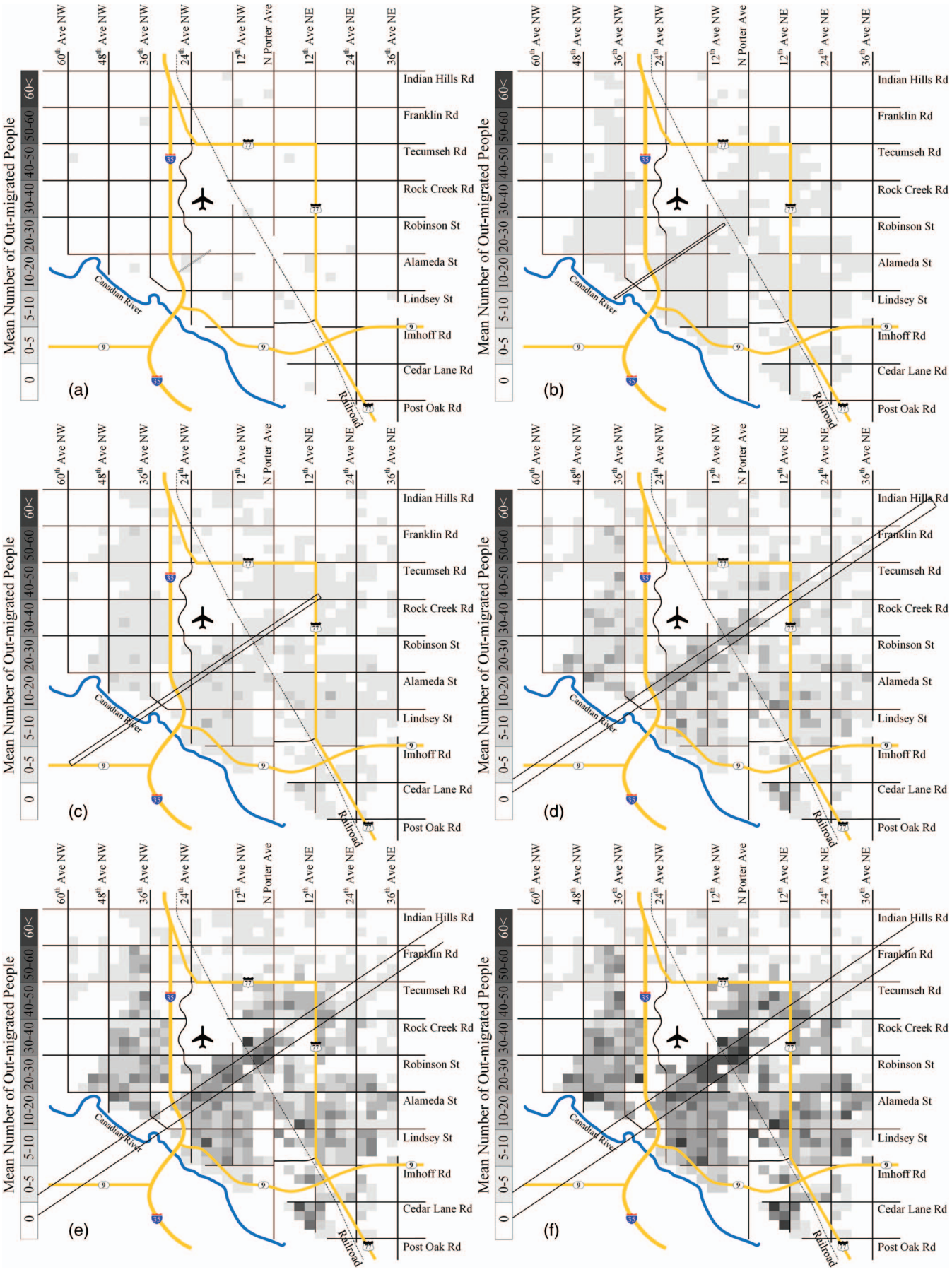

Fig. 11. (Color) Mean number of outmigrated people in each residential grid—the tornado paths with the mean length and width are shown in each case: (a) EF0; (b) EF1; (c) EF2; (d) EF3; (e) EF4; (f) EF5

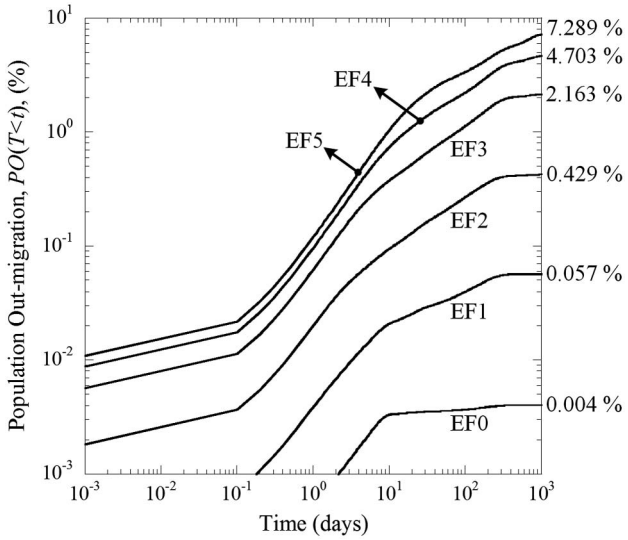

Fig. 12. Population outmigration after tornadoes with the path center and direction shown in Fig. 3 and with different intensities

Acknowledgments

The work presented in this paper was supported by the National Science Foundation (NSF) under Grant No. CMMI-1452725. This support is gratefully acknowledged. All views expressed in this paper are those of the authors and do not necessarily reflect the views of the NSF.

References

Alexander, D. E. (2013). "Resilience and disaster risk reduction: An etymological journey." *Nat. Hazards Earth Syst. Sci.*, 13(11), 2707–2716.

Attoh-Okine, N. O., Cooper, A. T., and Mensah, S. A. (2009). "Formulation of resilience index of urban infrastructure using belief functions." *IEEE Syst. J.*, 3(2), 147–153.

Ayyub, B. M. (2014). "Systems resilience for multihazard environments: Definition, metrics, and valuation for decision making." *Risk Anal.*, 34(2), 340–355.

Ayyub, B. M. (2015). "Practical resilience metrics for planning, design, and decision-making." *ASCE-ASME J. Risk Uncertainty Eng. Syst. Part A: Civ. Eng.*, 1(3), 04015008.

Baker, E. J. (1991). "Hurricane evacuation behavior." *Int. J. Mass Emergencies Disasters*, 9(2), 287–310.

Belcher, J. C., and Bates, F. L. (1983). "Aftermath of natural disasters: Coping through residential mobility." *Disasters*, 7(2), 118–128.

Boruff, B. J., Easoz, J. A., Jones, S. D., Landry, H. R., Mitchem, J. D., and Cutter, S. L. (2003). "Tornado hazards in the United States." *Climate Res.*, 24(2), 103–117.

Bruneau, M., et al. (2003). "A framework to quantitatively assess and enhance the seismic resilience of communities." *Earthquake Spectra*, 19(4), 733–752.

Bruneau, M., and Reinhorn, A. (2007). "Exploring the concept of seismic resilience for acute care facilities." *Earthquake Spectra*, 23(1), 41–62.

Chang, S. E., and Shinozuka, M. (2004). "Measuring improvements in the disaster resilience of communities." *Earthquake Spectra*, 20(3), 739–755.

Cimellaro, G. P., Reinhorn, A. M., and Bruneau, M. (2010). "Framework for analytical quantification of disaster resilience." *Eng. Struct.*, 32(11), 3639–3649.

Drabek, T. E., and Key, W. H. (1984). *Conquering disasters: Family recovery and long-term consequences*, Irvington Publishers, New York.

FEMA (Federal Emergency Management Agency). (2003). "Multi-hazard loss estimation methodology–earthquake model. HAZUS-MH-MR4 technical manual." Dept. of Homeland Security, Washington, DC.

Fothergill, A., and Peek, L. (2015). *Children of Katrina*, Univ. of Texas Press, Austin, TX.

Gladwin, H., and Peacock, W. G. (1997). "Warning and evacuation: A night for hard houses." *Hurricane Andrew: Ethnicity, gender, and the sociology of disasters*, W. G. Peacock, B. H. Morrow, and H. Gladwin, eds., Routledge, New York, 52–74.

Henry, D., and Ramirez-Marquez, J. E. (2012). "Generic metrics and quantitative approaches for system resilience as a function of time." *Reliab. Eng. Syst. Saf.*, 99, 114–122.

Koliou, M., Masoomi, H., and van de Lindt, J. W. (2017). "Performance assessment of tilt-up big-box buildings subjected to extreme hazards: Tornadoes and earthquakes." *J. Perform. Constr. Facil.*, 10.1061/(ASCE)CF.1943-5509.0001059, 04017060.

Lee, S., Ham, H. J., and Kim, H. J. (2013). "Fragility assessment for cladding of industrial buildings subjected to extreme wind." *J. Asian Archit. Build. Eng.*, 12(1), 65–72.

Limbourg, P., Kochs, H., Echtle, K., and Eusgeld, I. (2007). "Reliability prediction in systems with correlated component failures—An approach using copulas." *ARCS Workshop Dependability and Fault Tolerance*, VDE, Zürich, Switzerland, 55–62.

Lin, Y. (2009). "Development of algorithms to estimate post-disaster population dislocation: A research-based approach." Ph.D. dissertation, Texas A&M Univ., College Station, TX.

Lindell, M. K., Perry, R. W., Prater, C., and Nicholson, W. C. (2006). *Fundamentals of emergency management*, FEMA, Washington, DC.

Lindell, M. K., and Prater, C. S. (2003). "Assessing community impacts of natural disasters." *Nat. Hazards Rev.*, 10.1061/(ASCE)1527-6988(2003)4:4(176), 176–185.

López, A. L., Rocha, L. E. P., Escobedo, D. L., and Sesma, J. S. (2009). "Reliability and vulnerability analysis of electrical substations and transmission towers for definition of wind and seismic damage maps for Mexico." *Proc., 11th Americas Conf. on Wind Engineering*, San Juan, PR.

MAEC (Mid-America Earthquake Center). (2006). "MAEviz software." ⟨http://mae.cee.illinois.edu/software/software_maeviz.html⟩ (May 2016).

Masoomi, H., and van de Lindt, J. W. (2016). "Tornado fragility and risk assessment of an archetype masonry school building." *Eng. Struct.*, 128, 26–43.

Masoomi, H., and van de Lindt, J. W. (2017). "Tornado community-level spatial damage prediction including pressure deficit modeling." *Sustainable Resilient Infrastruct.*, 2(4), 179–193.

Masoomi, H., and van de Lindt, J. W. (2018). "Restoration and functionality assessment of a community subjected to tornado hazard." *Struct. Infrastruct. Eng.*, 14(3), 275–291.

Mitchell, C. M., Esnard, A.-M., and Sapat, A. (2012). "Hurricane events, population displacement, and sheltering provision in the United States." *Nat. Hazards Rev.*, 10.1061/(ASCE)NH.1527-6996.0000064, 150–161.

Nan, C., and Sansavini, G. (2017). "A quantitative method for assessing resilience of interdependent infrastructures." *Reliab. Eng. Syst. Saf.*, 157, 35–53.

Omer, M., Nilchiani, R., and Mostashari, A. (2009). "Measuring the resilience of the trans-oceanic telecommunication cable system." *IEEE Syst. J.*, 3(3), 295–303.

Ouyang, M., and Dueñas-Osorio, L. (2014). "Multi-dimensional hurricane resilience assessment of electric power systems." *Struct. Saf.*, 48, 15–24.

Ouyang, M., Dueñas-Osorio, L., and Min, X. (2012). "A three-stage resilience analysis framework for urban infrastructure systems." *Struct. Saf.*, 36, 23–31.

Pant, R., Barker, K., Ramirez-Marquez, J. E., and Rocco, C. M. (2014). "Stochastic measures of resilience and their application to container terminals." *Comput. Ind. Eng.*, 70, 183–194.

Peacock, W. G., and Girard, C. (1997). "Ethnicity and segregation." *Hurricane Andrew: Ethnicity, gender and the sociology of disaster*, W. G. Peacock, B. H. Morrow, and H. Gladwin, eds., Routledge, New York, 191–205.

Platt, S., Brown, D., and Hughes, M. (2016). "Measuring resilience and recovery." *Int. J. Disaster Risk Reduct.*, 19, 447–460.

Reed, D. A., Kapur, K. C., and Christie, R. D. (2009). "Methodology for assessing the resilience of networked infrastructure." *IEEE Syst. J.*, 3(2), 174–180.

Standohar-Alfano, C. D., and van de Lindt, J. W. (2014). "Empirically based probabilistic tornado hazard analysis of the United States using 1973–2011 data." *Nat. Hazards Rev.*, 10.1061/(ASCE)NH.1527-6996.0000138, 04014013.

Weber, L., and Peek, L. (2012). *Displaced: Life in the Katrina Diaspora*, Univ. of Texas Press, Austin, TX.

Whitehead, J. C. (2005). "Environmental risk and averting behavior: Predictive validity of jointly estimated revealed and stated behavior data." *Environ. Resour. Econ.*, 32(3), 301–316.

Whitehead, J. C., Edwards, B., Van Willigen, M., Maiolo, J. R., Wilson, K., and Smith, K. T. (2000). "Heading for higher ground: Factors affecting real and hypothetical hurricane evacuation behavior." *Global Environ. Change Part B: Environ. Hazards*, 2(4), 133–142.

Xiao, Y., and Van Zandt, S. (2011). "Building community resiliency: Spatial links between household and business post-disaster return." *Urban Stud.*, 49(11), 2523–2542.